

Electron tunneling across an interfacial water layer inside an STM junction: tunneling distance, barrier height and water polarization effect

J.R. Hahn, Y.A. Hong, H. Kang*

Department of Chemistry, Pohang University of Science and Technology, Pohang, Gyeongbuk 790-784, South Korea
 (Fax: +82-562/279-3399, E-mail: surfion@vision.postech.ac.kr)

Received: 25 July 1997/Accepted: 1 October 1997

Abstract. We have studied electron tunneling characteristics across an aqueous STM capacitor junction by measuring the tunneling current and local barrier height as functions of junction distance and applied bias voltage for HOPG, Au and TaTe₂ surfaces in air. The electron tunneling distance ranges from 7–20 Å when the junction resistance is of the order of 10⁸ Ω. We suggest that the unusually low value of the barrier height (< 1.5 eV) originates from the three-dimensional nature of the electron tunneling through the interfacial water layer present inside the junction. An asymmetric variation in barrier height is observed with respect to the applied bias voltage at a junction distance of water monolayer thickness, which reflects the polarization of the water layer on the surface.

The nature of the interfacial water layer and its response to electron transmission are related to many important phenomena in the physical sciences. However, current knowledge on this subject is far from complete. Theoretical considerations [1–3] predict that water molecules are polarized at a charged interface by breaking the bulk structure maintained by hydrogen bonding network under an interfacial electric field of the order of 10⁷ V/cm. Spectroscopic studies [4, 5] give evidence for a disrupted hydrogen bonding network in the first layer of water on a metal electrode. X-ray scattering studies [6, 7] have measured the spacing between the Ag electrode surface and the first layer of water and found that water molecules flip their average dipole orientation upon changing the polarity of the electrode potential.

Scanning tunneling microscopy (STM) can, in principle, be used to characterize the interfacial water and its electron transmission property. An electrochemical environment [8–10] or humid atmosphere [11–14] provides an STM junction filled with water, in the latter case condensed from atmospheric moisture [13, 14]. In the aqueous STM studies, however, many aspects are still not well resolved or perhaps have not been given enough detailed consideration. For example,

water inside an STM junction greatly increases the tunneling distance compared with that in ultrahigh vacuum (UHV) [8]. The local barrier height for electron tunneling (ϕ) is unusually low in water [8–12, 15] compared with UHV [16–19]. These phenomena should somehow be related to the physics of electron transfer across interfacial water, but this remains uncertain at present. In this work, we examine electron tunneling across the interfacial water layer present inside a capacitor junction composed of an STM tip and sample surface in air. The junction distance is accurately controlled to water monolayer thickness, and the tunneling current (I) and ϕ are investigated as functions of junction distance and applied bias voltage.

1 Experimental section

The experiment was performed using an air STM instrument of home-built design and RHK control electronics. The tip was either a W wire etched by an electrochemical method or a mechanically cut Pt-Ir wire. The samples were Au, HOPG and TaTe₂. The Au(111) terrace plane was prepared by flame melting of a gold wire. HOPG and TaTe₂, materials of layered structure, were cleaved to expose their fresh surface before each experiment.

We performed the ϕ measurements using the a.c. modulation method [20]. An a.c. voltage was applied to the z-piezo drive so that the tip oscillates at a small amplitude ($\Delta z < 1$ Å) at a frequency of 1–10 kHz. The induced modulation of the tunneling current, ΔI , was detected using a lock-in technique. The modulation frequency was within the bandwidth of an $I - V$ converter [21]. A two-dimensional ϕ image of an HOPG surface with atomic resolution was routinely obtainable in this manner, and it was in phase with the corresponding topographic image, as reported earlier [20]. ϕ was also measured as a function of tip-sample separation distance, s , by slowly displacing the tip position, z , perpendicular to the surface. The modulated tunneling current, dI/dz , was recorded simultaneously with the average tunneling current using two input channels. The tip-approach experiment gives

* To whom correspondence should be addressed

$\phi - z$ information, which, except for very short gap distances, is basically equivalent to $\phi - s$ information.

2 Results and discussion

2.1 Tunneling distance through an interfacial water layer

Figure 1 shows the results of $\phi - z$ measurement on HOPG, Au(111) and TaTe₂ surfaces with a W tip at negative sample bias voltage. We first take a topographic STM image of a surface in order to ensure that the tip produces atomic resolution. The tunneling resistance for topographic imaging is depicted by the arrow, and is of the order of $R_t \sim 10^8 \Omega$. The tip is then retracted by several Å from the preset imaging position, and then ϕ and I are measured while the tip is slowly pushed toward the sample until mechanical contact occurs. The definition of mechanical contact is presented in the next paragraphs. The common $\phi - s$ features for the three samples are: (i) ϕ stays fairly constant at about 0.7–1.3 eV for large s and decreases only slightly with decreasing s ; (ii) as the tip approaches the surface, to within 3 Å, ϕ drops suddenly to zero. A feature that is different for the three samples is the distance of tip travel between the positions for the initial imaging ($R_t \sim 10^8 \Omega$) and the ϕ drop (contact). The initial tunneling distance ranges from 7–20 Å, for which there exists a qualitative trend of increasing in the order of HOPG < Au < TaTe₂.

Also shown in Fig. 1 is the tunneling current recorded simultaneously with the $\phi - z$ data. The current data are plotted for $\ln I$ versus z . For vacuum tunneling such a plot gives linear behavior, because $I/V_t \propto \exp(-\sqrt{\phi}s)$, where a square potential barrier is assumed and V_t is the voltage across an STM junction. The plot of Fig. 1 exhibits two approximately linear regions, which break at the position of the ϕ drop to zero.

From the data of Fig. 1, we suggest that tip-surface contact occurs at the position where ϕ drops to zero and the $\ln I$ curve breaks. Upon repulsive contact, the surface and/or the tip become pushed in, resulting in lowering of an experimentally measured barrier height, ϕ_{exp} , as described by (1) [20].

$$\sqrt{\phi_{\text{exp}}} = -\frac{d \ln I}{dz} = -\frac{d \ln I}{ds} \frac{ds}{dz} = \sqrt{\phi} \frac{ds}{dz}, \quad (1)$$

where dz is the tip displacement and ds is the corresponding change of gap distance. The ratio ds/dz represents an elasticity measure for a tip-sample system. For small Δz and during initial contact ds/dz can be reduced almost to zero (Sect. 2.2). In this sense, the sudden drop in the $\phi_{\text{exp}} - z$ curves is assigned to a repulsive contact between the tip and the bare surface. Another indication for the tip-surface contact comes from the plot of $\ln I$ vs. z . In a vacuum tunneling study with combined tunneling current and force gradient measurement [22], two different contact behaviors have been observed, depending on tip-sample combination. A plot of $\ln I$ vs. z bends downward upon contact between an Ir tip and an Al sample, and repulsive interaction has been detected. For an Ir tip-Ir sample system, on the other hand, an upward jump has been observed upon contact, which has been attributed to the attractive, adhesive nature of contact. The curves of Fig. 1 resemble the Ir tip-Al sample system, indicating repulsive contact. The repulsive nature of the W-surface

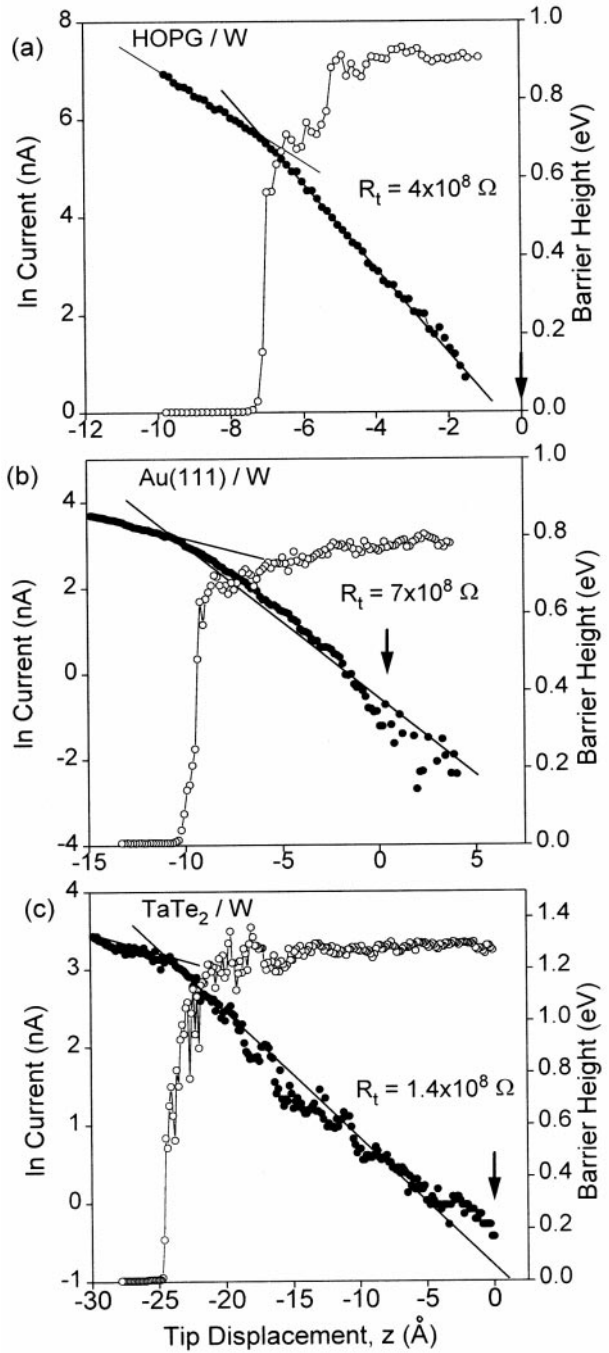


Fig. 1a–c. Tunneling current (solid circles) and local barrier height (open circles) simultaneously measured as a function of tip displacement perpendicular to surface. The tunneling current, shown at the left-hand side, is on a logarithmic scale. The barrier height is shown at the right-hand side. The straight lines are to visualize the two linear regions of the $\ln I$ curves. The tunneling resistance at the initial tip position ($z = 0$) is indicated by the arrow. **a** W tip and HOPG surface for the initial scanning condition of sample bias -0.2 V and current 0.5 nA. **b** W tip and Au(111) surface for -0.2 V and 0.3 nA. **c** W tip and TaTe₂ surface for 0.1 V and 0.7 nA

interaction is reasonable because the W tip in air is covered with oxides. A recent STM contact study [18] has suggested measuring tunneling conductance instead of tunneling current in order to judge the contact position. This is because the voltage across an STM junction (V_t) can become smaller than the

external bias voltage when the junction resistance is reduced upon near-contact to the surface. In the present case, however, both tunneling current and conductance yield the same result because an $I-V$ converter with small input impedance is used [21]. The positions for the ϕ drop and the break in the $\ln I$ curve coincide each other within 1–2 Å, which indicates the accuracy in defining the contact point.

In order to check the validity of the $\phi-z$ data obtained by the tip-approach experiment, we have performed ϕ measurement using a different mode. This time we fixed the equilibrium distance of the tip and change the amplitude of modulation, Δz . Figure 2 shows the result of this experiment for a W tip-HOPG system. As Δz is increased to about 14 Å, which is twice the value of the equilibrium gap distance (7 Å), ϕ_{exp} suddenly drops. At this modulation amplitude, the tip apparently starts touching and pushing the surface at one end of its z -modulation, resulting in partial lowering of ϕ_{exp} .

The results of the tip-surface approach study reveal that the tunneling distance is very large for normal scanning conditions of air STM ($s = 7\text{--}20$ Å at $R_t \sim 10^8 \Omega$) compared with that for UHV STM ($s = 3\text{--}5$ Å). It is obvious that the STM junction is filled with a layer of non-insulating materials, most likely water molecules condensed from atmospheric moisture, as has been suggested in previous studies [11–14]. The tunneling distance measured in this work agrees with the result for aqueous phase tunneling, a value of $s \leq 10$ Å at $R_t = 10^7 \Omega$ has been deduced from $I-z$ characteristics for an Au tip and an Au sample in an electrochemical environment [8]. A study of adsorbed water films [14] has found that a water bridge can be formed as thick as several hundred Å between the STM tip and a hydrophilic Pt/C surface. On an Au surface no comparable phenomenon was observed for atmospheric humidity < 75% [14]. We consider that the hydrophobic nature of an Au surface prohibits formation of such thick water layers on the surface. Nonetheless, a thinner water bridge (~ 10 Å) can apparently be formed between the tip and the surface.

The tunneling distance through an interfacial water layer will depend on several factors, possibly including the elec-

tronic density of states of the tip and the surface, their hydrophilicity, and the nature of the water films. Among the three surfaces examined, TaTe₂ exhibits the largest tunneling distance. TaTe₂ is a transition metal dichalcogenide with its cleaved surface exposing Te atoms [23]. This surface should be very hydrophilic, as we observe hygroscopic degrading of TaTe₂ sample in ambient air. The large tunneling distance for TaTe₂ is therefore consistent with a dense and thick layer of water formed on the hydrophilic surface.

2.2 Surface deformation by tip-induced force

The ϕ value for aqueous STM experiments is extremely small (0.7–1.3 eV) compared with that in vacuum, and this phenomenon is widely known [8–12]. However, the origin of the ϕ lowering remains controversial. It has been suggested [11] that the tip pressure can be mediated by the water layer on a surface, resulting in low ϕ_{exp} . An opposite interpretation has been reported [12]: that the tip-sample force does not play a significant role in the lowering of ϕ_{exp} on gold in air. In this section we address the effect of tip-pressure on the lowering of ϕ_{exp} .

The observed variation of ϕ_{exp} can be quantitatively modeled by assuming that the force between a tip and a sample follows a Morse curve [11, 17, 24]. Figure 3 shows the simulation result for $\phi-s$ variation and surface deformation. The solid circles represent the experimental $\phi-s$ data obtained from a W tip-HOPG system. In the simulation, we match ϕ to the experimental value for large gap distances (0.9 eV) and the following parameters are used: decay rate for wavefunction of 0.47 Å^{-1} , Young's modulus of 3.4×10^{12} and $7 \times 10^{10} \text{ dyne/cm}^2$ for tip and sample, respectively [25], and tip radius of 50 Å. These parameters are thought to be reasonable for a W tip and an HOPG surface. The agreement is quite good between the experiment and the simulation. The simulation reveals several features for tip-surface interaction. (i) For tip-sample separation of $s > 3$ Å, ϕ stays constant at an assumed value of 0.9 eV. The interaction is attractive in

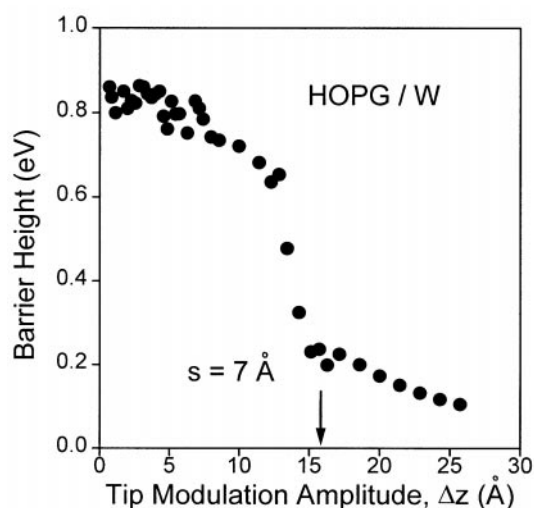


Fig. 2. Tunneling barrier height measured by changing the amplitude of tip modulation at a fixed equilibrium gap distance (7 Å)

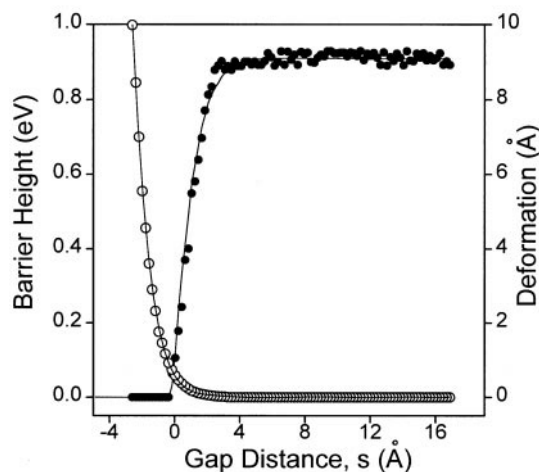


Fig. 3. Model calculation for surface deformation and the resulting variation in barrier height induced by tip-surface interaction forces. The solid circles represent the experimental barrier height obtained from a W tip-HOPG system. See the text for calculation details

this normal R_t region, but the variation in ϕ coming from the attractive interaction is very small because of the negligible surface deformation ($< 0.1 \text{ \AA}$). The effect of attractive forces on ϕ can be somewhat better highlighted if one uses a tip of smaller radius. (ii) As the gap distance decreases, to within 2 \AA , the repulsive force effect becomes more dominating. The repulsive force is very strong at short range and results in lowering of ϕ by surface deformation, as described by (1). (iii) A further decrease of the gap distance causes ϕ to drop almost to zero, representing mechanical contact between the tip and the surface [19, 26].

The present simulation does not include interfacial water molecules, but still gives good agreement with the experimental result. This indicates that the interfacial water layer does not mediate the tip pressure [11] on a surface to any significant degree for water layer thicknesses of several \AA or larger. It is clearly shown by experimental observation that ϕ_{exp} stays constant at the corresponding gap distances. We mention at this stage that the elastic deformation model reproduces this result only for the negative sample bias case. It will be shown in Sect. 2.3 that ϕ increases with decreasing s when the sample bias is positive. This bias polarity effect has different origins from the elastic deformation, but we just point out here that the ϕ increase for small s also opposes the earlier proposal of tip-induced pressure effect [11].

2.3 Bias voltage dependence of tunneling barrier

While the $\phi - z$ variation for negative sample bias is characterized by the curve features of Fig. 1, drastically different behavior is observed when the bias polarity is changed to positive. Figure 4 shows the $\phi - z$ curves obtained by changing the polarity of sample bias in the sequence -0.2 V (a), $+0.2 \text{ V}$ (b) and -0.2 V (c) for a W tip-Au sample system. For positive sample bias, ϕ sharply increases to exceed several eV upon close approach of a tip to a surface. The ϕ peaking occurs at the gap distance of $0-3 \text{ \AA}$, and then suddenly drops to zero upon contact. The ϕ values at large gap distances are similar for both positive and negative sample biases. In some cases a slightly higher value ($1.0-1.5 \text{ eV}$) is measured for positive sample bias. The ϕ dependency on applied bias voltage is reversible, as illustrated in Fig. 4; the corresponding $\phi - z$ features reappear even after changing the bias polarity back and forth several times. We have performed the ϕ dependence study on bias voltage with other tip-surface combinations, including W-HOPG and Pt/Ir-HOPG. The results are qualitatively similar to Fig. 4, i.e. the $\phi - z$ curves peak for positive sample bias and for a short gap distance, while they do not for negative bias. The height of the ϕ peak increases as the sample bias potential is increased toward positive, from 2.3 eV at a sample bias of $+0.02 \text{ V}$ to 6.8 eV at $+0.6 \text{ V}$ for the case of a W-HOPG system. For negative sample bias voltages, ϕ peaking is not observed as we decrease the voltage to -0.6 V .

The above-mentioned $\phi - z$ results can be summarized by three features. (i) ϕ variation with bias potential is most pronounced at a gap width of $0-3 \text{ \AA}$. (ii) ϕ stays constant at large gap distances for all bias potentials. (iii) The height of the ϕ peak increases with increasing applied voltage for positive sample bias.

As a note for experiment, we would like to mention that the ϕ peaking occurs only for very small s , and accordingly

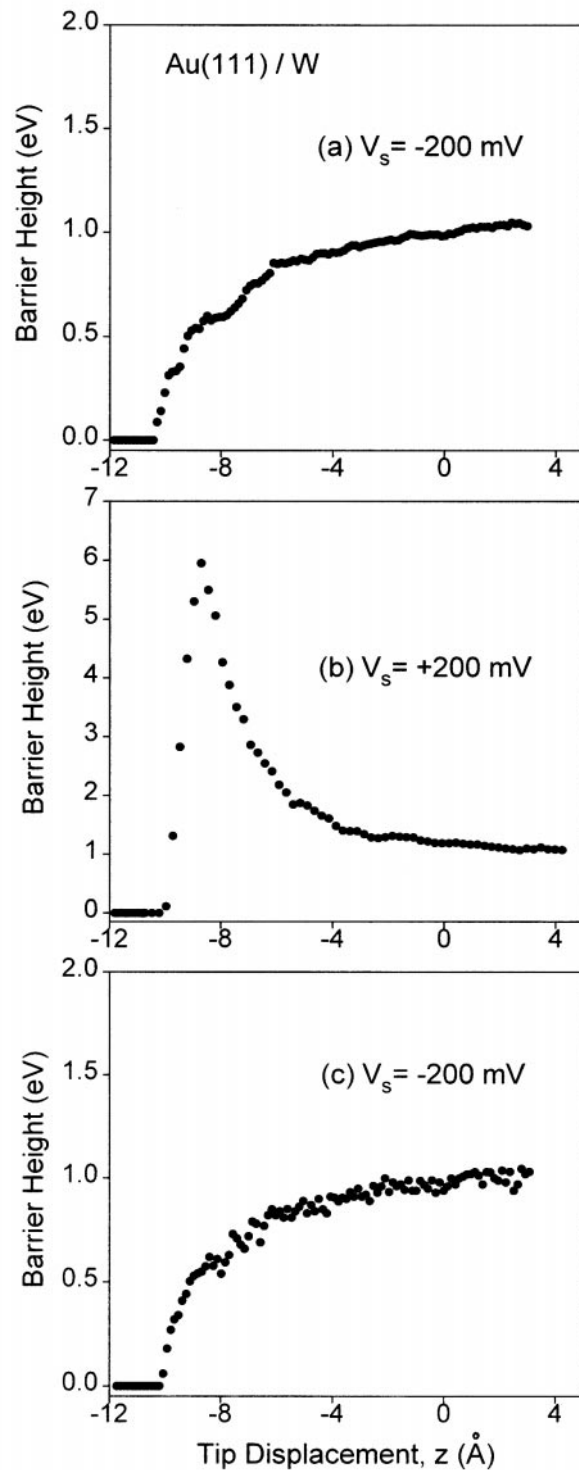


Fig. 4. Variation of the $\phi - z$ curve with external bias polarity for a W tip-Au(111) system. V_s represents the potential applied at the sample with respect to the grounded tip. Measurement was done in the sequence a, b and c. ϕ peaking occurs only for a positive sample bias and at a gap distance of $0-3 \text{ \AA}$

for small R_t . In some STM experiments [27], s is varied by changing the applied bias voltage while keeping I constant. Extreme caution will be needed to observe ϕ peaking in such a mode of experiment, because in order to attain the neces-

sary gap distance ($s < 3 \text{ \AA}$) the applied voltage will become inevitably too small.

The observation that the asymmetric ϕ peaking is independent of the materials of the sample and tip indicates that its origin is different from the electronic nature of the tip and sample surface. The asymmetric ϕ peaking cannot be explained by the existing models for electron tunneling in vacuum nor by the model for elastic deformation of surface. We are forced to conclude that the $\phi - z$ feature is related to the interfacial water layer present inside the STM junction. However, we exclude the possibility of an aqueous electrochemical reaction contributing to the ϕ peaking because of the fact that peaking occurs reversibly and at bias voltages as low as $+0.02 \text{ V}$, a value lower than the reversible potential for any possible surface electrochemical reaction. For example, the reversible potential for H_2O dissociation is 1.23 V .

Recently, it has been suggested [28–31] that electron tunneling through a molecularly thin water layer needs to be understood in relation to the detailed molecular structure of the layer, i.e. three-dimensional tunneling phenomena are to be incorporated. A simple linear tunneling model through a structureless dielectric continuum is unrealistic for such a case. A recent calculation [31] of the electron transmission probability has predicted similar asymmetric behavior of electron tunneling through a 10 \AA water layer polarized by an electric field between two parallel capacitor plates. The tunneling probability in this calculation is 4–5 orders of magnitude larger when an electron enters from the hydrogen face of polarized water molecules than from the oxygen face. In the following text, we offer the polarization of interfacial water molecules inside an STM junction as a viable explanation for the observed asymmetric ϕ peaking.

First, inside an STM capacitor junction, water molecules are expected to be polarized because the internal electrical field strength is $1 \times 10^6 - 3 \times 10^7 \text{ V/cm}$ for a junction distance of 2 \AA and bias voltages of $0.02 - 0.6 \text{ V}$, if we ignore the dielectric contribution of water. Recent X-ray scattering experiments [6, 7] have observed water polarization, or formation of the dipole-oriented layer, on an $\text{Ag}(111)$ electrode surface. The first-layer water molecules on this surface reorient from oxygen-up to oxygen-down as the electrode charge changes from negative to positive. Second, when the water polarization occurs inside an STM junction, the situation can be quite different from the two parallel metal plates employed in the model calculation [31]. The degree of polarization is smaller at the apex atom of the STM tip than on a flat sample surface, according to electrostatic considerations, because the tip atom resembles a partial point charge. Due to the weaker electrostatic field around the tip atom, water molecules tend to form a loosely polarized hydration shell around the atom rather than a well-oriented layer [32]. Third, X-ray scattering studies [6, 7] have shown that a positively biased Ag electrode surface more strongly polarizes the first-layer water molecules than a negatively charged surface. On a positively biased surface, severe compression occurs in two dimensions for the first-layer water molecules. Similarly, we expect a higher degree of polarization and lateral compression in the water layer on the positively biased surface of an STM junction. This means that the formation of a dipole-oriented layer depends largely on the potential polarity applied at the flat sample surface, while the tip has a smaller effect on water polarization. Consequently, water polarization becomes asymmetric with

respect to the bias voltage applied at the STM junction. The polarized and compressed water layer reduces the probability for electron tunneling through the near space of H atoms of water molecules [30], thus imposing a high tunneling barrier, which is in agreement with experimental observation.

3 Conclusions

From the $I - z$ and $\phi - z$ characteristics measured on HOPG, Au and TaTe_2 surfaces in air, we conclude that the electron tunneling distance ranges $7 - 20 \text{ \AA}$ for normal scanning conditions ($R_t \sim 10^8 \Omega$). Precise control of the STM junction at molecular distances allows us to probe ϕ as a function of interfacial water thickness. We suggest that the unusually low value of ϕ ($< 1.5 \text{ eV}$) observed for the large gap distance originates from the three-dimensional nature of electron tunneling through several water layers. On the other hand, the water-mediated tip pressure does not play a major role in ϕ lowering in this case. Asymmetric ϕ peaking is observed with respect to the applied bias voltage when the gap distance approaches the water monolayer thickness. We attribute this asymmetric behavior to the polarized nature of the first-layer water molecules, i.e. to the formation of a dipole-oriented layer on a positively charged sample surface.

Acknowledgements. We thank Professor Sung-Jin Kim for providing the TaTe_2 sample. This work was supported in part by the Korea Science and Engineering Foundation (CMS), the Ministry of Education of Korea, and BSRI funds.

References

1. W.R. Fawcett, S. Levine, R.M. deNobriga, A.C. McDonald: *J. Electroanal. Chem.* **111**, 163 (1980)
2. G. Alosi, M.L. Foresti, R. Guidelli, P. Barnes: *J. Chem. Phys.* **91**, 5592 (1989)
3. G. Nagy, K. Heininger: *J. Electroanal. Chem.* **327**, 25 (1992)
4. T.T. Chen, R.K. Chang: *Surface Sci.* **158**, 325 (1985)
5. J.E. Pemberton, S.L. Joa: *J. Electroanal. Chem.* **378**, 149 (1994)
6. M.F. Toney, J.N. Howard, J. Richer, G.L. Borges, J.G. Gordon, O.R. Melroy, D.G. Wiesler, D. Yee, L.B. Sorensen: *Nature* **368**, 444 (1994)
7. M.F. Toney, J.N. Howard, J. Richer, G.L. Borges, J.G. Gordon, O.R. Melroy, D.G. Wiesler, D. Yee, L.B. Sorensen: *Surface Sci.* **335**, 326 (1995)
8. M. Bingelli, D. Carnal, R. Nyffenegger, H. Siegenthaler, R. Christoph, H. Rohrer: *J. Vac. Sci. Technol. B* **9**, 1985 (1991)
9. W. Haiss, D. Lackey, J.K. Sass, K.H. Besocke: *J. Chem. Phys.* **95**, 2193 (1991)
10. G. Nagy: *J. Electroanal. Chem.* **409**, 19 (1996)
11. H.J. Mamin, E. Ganz, D.W. Abraham, R.E. Thomson, J. Clarke: *Phys. Rev. B* **34**, 9015 (1986)
12. S.C. Meepagala, F. Real: *Phys. Rev. B* **49**, 10761 (1994)
13. D.A. Grigg, P.E. Russell, J.E. Griffith: *J. Vac. Sci. Technol. A* **10**, 680 (1992)
14. M. Heim, R. Eschrich, A. Hillebrand, H.F. Knapp, R. Guckenberger, G. Cevc: *J. Vac. Sci. Technol. B* **14**, 1498 (1996)
15. G. Repphun, J. Halbritter: *J. Vac. Sci. Technol. A* **13**, 1693 (1995)
16. J.K. Gimzewski, R. Moller: *Phys. Rev. B* **36**, 1284 (1987)
17. C.J. Chen, R.J. Hamers: *J. Vac. Sci. Technol. B* **9**, 230 (1991)
18. L. Olesen, M. Brandbyge, M.R. Sorensen, K.W. Jacobsen, E. Laegsgaard, I. Stensgaard, F. Besenbacher: *Phys. Rev. Lett.* **76**, 1485 (1996)
19. L. Olesen, E. Lagsgaard, I. Stensgaard, F. Besenbacher: *Phys. Rev. Lett.* **72**, 2251 (1994)
20. R. Wiesendanger: *Scanning Probe Microscopy and Spectroscopy* (Cambridge University Press, Cambridge 1994)
21. RHK Technology, Inc.: A bandwidth of 20 kHz and an effective input impedance of $4 \text{ k}\Omega$

22. U. Dürig, O. Züger, L.C. Wang, H.J. Kreuzer: *Europhys. Lett.* **23**, 147 (1993)
23. S.-J. Kim S.-J. Park, H.-J. Oh, I.C. Jeon, S. Song: *Bull. Korean Chem. Soc.* **15**, 1098 (1994)
24. J.M. Soler, A.M. Baro, N. Garcia, H. Rohrer: *Phys. Rev. Lett.* **57**, 444 (1986)
25. D.E. Gray: *American Institute of Physics Handbook*, 3rd edn (McGraw-Hill, New York 1972) pp. 2-67
26. U. Landman, W.D. Luedtke, N.A. Burnham, R.J. Colton: *Science* **248**, 454 (1990)
27. J. Pan, T.W. Jing, S.M. Lindsay: *J. Phys. Chem.* **98**, 4205 (1994)
28. W. Schmickler: *Nanoscale Probes of the Solid/Liquid Interface* (Kluwer, Amsterdam 1995) p. 5
29. R.N. Barnett, U. Landman, C.L. Cleveland, J. Jortner: *J. Chem. Phys.* **88**, 4429 (1988)
30. K.S. Kim, I. Park, S. Lee, K. Cho, J.Y. Lee, J. Kim, J.D. Joannopoulos: *Phys. Rev. Lett.* **76**, 956 (1996)
31. I. Benjamin, D. Evans, A. Nitzan: *J. Chem. Phys.* **106**, 1291 (1997); *ibid*, 6647
32. J.K. Sass, J.K. Gimzewski: *J. Electroanal. Chem.* **308**, 333 (1991)